



Available online at www.sciencedirect.com

ScienceDirect

Energy Procedia 154 (2018) 66–72

Energy

Procedia

www.elsevier.com/locate/procedia

Applied Energy Symposium and Forum, Carbon Capture, Utilization and Storage, CCUS 2018,
27–29 June 2018, Perth, Australia

Flow characteristics and dispersion during the vertical anthropogenic venting of supercritical CO₂ from an industrial scale pipeline

Xingqing Yan^a, Xiaolu Guo^a, Jianliang Yu^{a*}, Shaoyun Chen^b, Yongchun Zhang^b, Haroun Mahgerefteh^c, Sergey Martynov^c, Solomon Brown^c

^aSchool of Chemical Machinery and Safety, Dalian University of Technology, Dalian, 116024, China

^bSchool of Chemical Engineering, Dalian University of Technology, Dalian, 116024, China

^cDepartment of Chemical Engineering, University College London, London WC1E 7JE, UK

Abstract

Pressurized pipelines represent the most reliable and cost effective way of transporting captured CO₂ from fossil fuel-fired electricity generation plants for subsequent sequestration. Leakage of CO₂ through a small puncture is the most common form of pipeline failure during normal operation; such failures could lead to fracture. The study of pipeline depressurization and inventory dispersion behavior is of paramount importance for assessing the possibility of fracture propagation and the impact of CO₂ pipeline releases on the surrounding environment. A large-scale fully instrumented pipeline (258 m long, 233mm i.d.) was constructed to study the pressure response, phase transition and dispersion of gaseous, dense and supercritical phase CO₂ during vertical leakage through a 15 mm diameter orifice. The fluid pressures and temperatures in the pipeline were recorded to study the pressure response and phase transition inside the pipeline. Video cameras and CO₂ concentration sensors were used to monitor the formation of the visible cloud and the gas concentration distribution in the far-field. There was a “two cold, intermediate hot” phenomenon during the vertical release in the dense and supercritical release due to the dry ice particle accumulation near the orifice. The intersection of the jet flow and settling CO₂ mixture resulted in complex visible cloud forms in dense CO₂ release.

© 2018 The Authors. Published by Elsevier Ltd.

This is an open access article under the CC BY-NC-ND license (<http://creativecommons.org/licenses/by-nc-nd/4.0/>)

Selection and peer-review under responsibility of the scientific committee of the Applied Energy Symposium and Forum, Carbon Capture, Utilization and Storage, CCUS 2018.

Keywords: CO₂ leakage; Flow characteristic; Dispersion; Large-scale pipeline

1876-6102 © 2018 The Authors. Published by Elsevier Ltd.

This is an open access article under the CC BY-NC-ND license (<https://creativecommons.org/licenses/by-nc-nd/4.0/>)

Selection and peer-review under responsibility of the scientific committee of the Applied Energy Symposium and Forum, Carbon Capture, Utilization and Storage, CCUS 2018.

10.1016/j.egypro.2018.11.012

1. Introduction

Carbon capture and storage (CCS) involves capturing CO₂ from large industrial point sources of emission and then storing it in a reservoir instead of allowing its release to the atmosphere [1, 2]. CO₂ transportation is a key component of the CCS chain to transmit large amounts of CO₂ from emitter to storage site [3, 4]. The vent system represents an essential pressure-relief method for achieving the objectives of decreasing the pipeline pressure as soon as possible to safe range while preventing the expanded accidents and getting enough time to repair the pipeline during the planned vents or the leakage accidents [5]. In order to provide for safety, the block valves or the vent stations are typically required to be placed along the pipeline about 15 km maximum, per regulation such as US DOT CFR regulations. This prevents loss of pressure integrity of the entire pipeline, whereby sections can be isolated, limiting the amount of CO₂ released into the atmosphere [6, 7].

In the process of pipeline emptying, the large temperature drop and the dry ice jam will occur inside the main pipeline and vent tube due to the throttling effect while this can initiate the running-brittle fracture by a puncture [8, 9]. In the venting area, the releasable CO₂ may cause the potential for exposure of solid CO₂ particles and cryogenic exposure to the people within the range. Due to the relatively high density of gaseous CO₂ at ambient conditions the escaping CO₂ will rapidly concentrate in low-lying areas [10, 11]. Vent systems should be designed and located to ensure the potential safety consequences of a depressurization is within the acceptance criteria both in terms of occupational health and 3rd party risk [12].

Many experimental studies have recently been performed to analyze depressurization behavior and dispersion during the release of CO₂ from pipelines. Wareing et al. [13-15] introduced the venting of dense and gas phase CO₂ through a single, straight vertical vent pipe from high pressure pipes above ground within the framework of the COOLTRANS research program. The experimental data used in these releases was used to develop a CO₂ dispersion model. The near-field dispersion structures of such releases were predicted by a mathematical model against this experimental data. Han et al. [16, 17] studied liquid CO₂ flow characteristics in a 1/4 inch capillary tube used in 3 m and 10 m long. Temperature and pressure were measured in capillary tube to investigate the flow characteristics in the pipe. The experimental result showed that the phase change occurred just before CO₂ flow was exposed to ambient air for any tube length of this study. Xie et al. [18, 19] studied the vertical release of supercritical CO₂ from a 23 m long circulating pipe with a 30 mm inner diameter. A typical highly under-expanded jet flow structure was observed near the orifice.

This paper presents the flow characteristics and dispersion of supercritical phase CO₂ (99.9 % pure) during vertical venting through 4 m and 2 m long vent tubes with 50 mm diameter orifice. Fluid pressures and temperatures in the main pipeline and vent tube were recorded during release. Video cameras were used to monitor the formation of the visible cloud in the venting area. The experimental studies provide a detailed understanding of depressurization and dispersion behaviors during the venting of supercritical CO₂.

2. Experiments

Fig. 1 shows a schematic of experimental apparatus. The experimental apparatus consisted of two CO₂ injecting lines, a 257 m long main pipeline built in 16MnD low temperature carbon steel (inner diameters of 233 mm and 20 mm thickness), a 1 m long dual-disc blasting pipe and a vertical vent device built in grade 304 stainless steel. All the other details, instruments and experimental conductes were introduced by our previous papers [20-23].

In this paper the flow characteristics and dispersion of supercritical phase CO₂ released vertically through a 15 mm diameter orifice are reported. The initial experimental conditions and environmental conditions of three tests are presented in Table 1. The instrument types, numbers and locations of the selected instruments are given in Table 2.

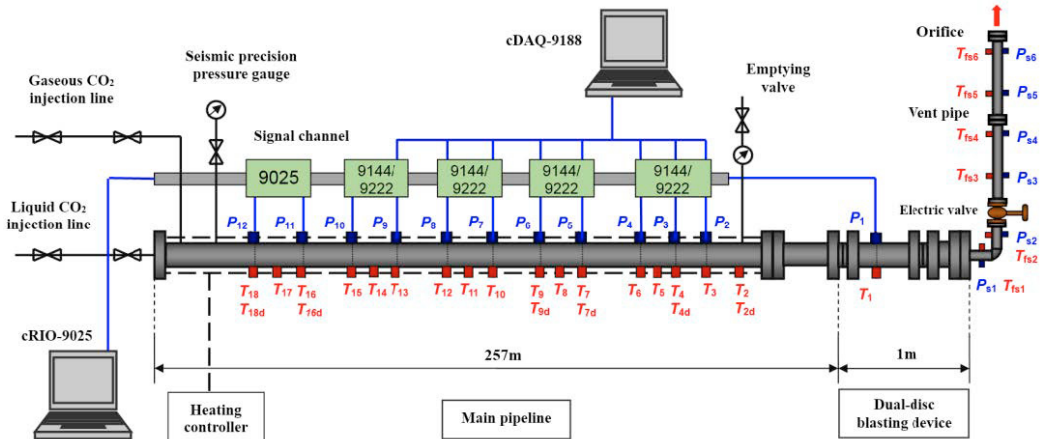


Fig. 1. Schematic and scene graph of experimental apparatus

Table 1. Experimental conditions and environmental conditions

Number	Test 1	Test 2
Pressure (MPa)	8.3	8.4
Temperature (°C)	38.0	37.0
Orifice (mm)	50	50
Inventory (tons)	4.0	5.1
Environmental pressure (kPa)	101.78	101.06
Environmental temperature (°C)	4.9	10.3
Humidity (%)	62.5	58.7
Wind speed (m/s)	0	1.0
Wind direction	-	47
Atmospheric stability	A	A

Table 2 Partial measurement point locations.

Temperature on top of the pipe	Temperature on bottom of the pipe	Wall temperature	Pressure	Distance from the orifice (m)
			P_1	0.74
T_{f2}	T_{f2d}	T_{w2}		7.4
			P_2	10.4
T_{f7}	T_{f7d}	T_{w7}	P_5	54.2
T_{f9}	T_{f9d}	T_{w9}	P_6	62.1
T_{f18}	T_{f18d}	T_{w18}	P_{12}	248.6

3. Results and Discussions

3.1 Pressure developments in the main pipeline and the vent pipe during depressurization

Fig. 2(a) and (b) show the evolutions of fluid pressures in the main pipeline and the vent pipe after rupture for tests 1 and 2. The total depressurization times for the two experiments were 412 s and 414 s respectively. After rupture, the pressures inside the main pipeline and the vent pipe in front of the operated valve fell from the initial pressure gradually. The pressures inside the vent pipe behind the operated valve increase firstly and then decrease. From the magnified regions of Fig. 2, it can be seen that at about 8 s after the valve opened, the pressure gradients among P_{s3} , P_{s4} , P_{s5} , and P_{s6} reach maximum. And at about 20 s after the valve opened, the pressure gradients among P_{s1} , P_{s2} , and P_{s3} reach maximum.

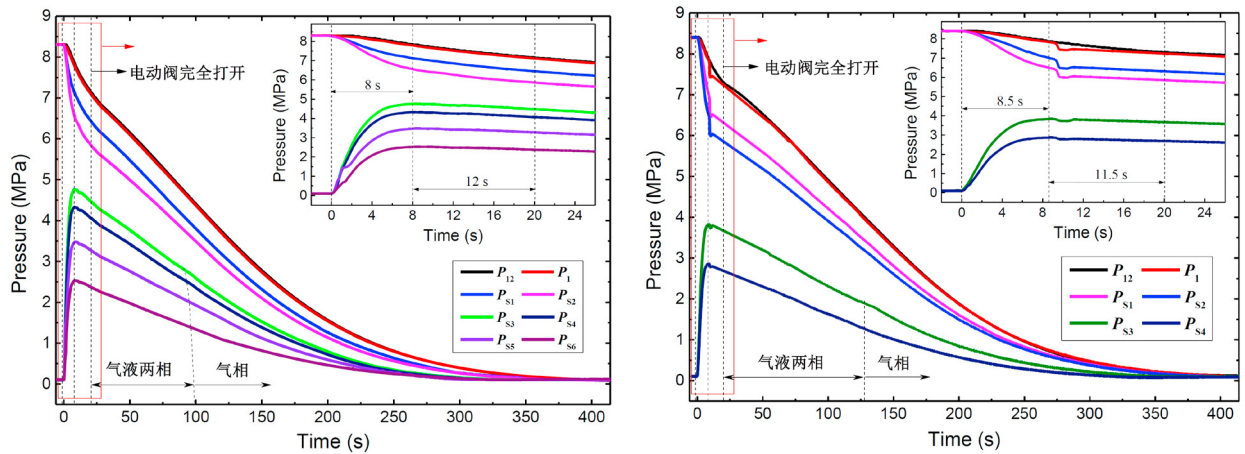


Fig. 2. Pressure evolutions for tests 1 and 2.

3.2 Phase transitions during pipeline depressurization

Fig. 3 (a) shows the evolution of CO₂ phase diagram in the main pipeline. After the valve opened, the supercritical CO₂ transformed into the gas-liquid phase when the pressure was lower than the critical pressure P_c . Phase changes of top and bottom fluid at the same distance from the vent orifice were exactly the same. As the pipe pressure and temperature continued to drop, the pressure and temperature points successively deviated from the saturation line into the gas phase area. This suggested that the transformation from the gas-liquid phase to the gaseous CO₂ started to appear from the vent orifice to the closed end of the pipeline.

Fig. 3 (b) shows the evolution of CO₂ phase diagram in the vent pipe. After the valve opened, the inventory properties of Tfs1-Ps1 and Tfs2-Ps2 in front of the valve inside the vent pipe passed through the supercritical region and into the gaseous region of the phase diagram following a parallel trajectory to the saturation line, indicating that the present phase was superheated gas. The phase transitions of Tfs3-Ps3, Tfs4-Ps4, Tfs5-Ps5, and Tfs6-Ps6 behind the vent valve in the vent pipe were complex.

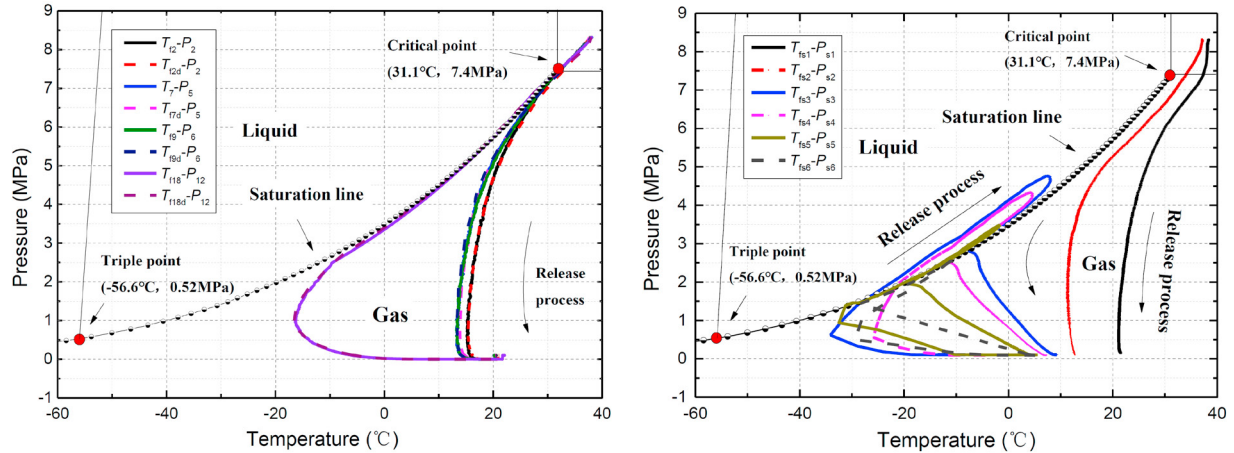


Fig. 3 Pressure-temperature developments in the main pipe and the vent pipe for test 1

Fig. 4 (a) and (b) shows the evolution of the Test 2 fluid pressure and temperature plotted on the CO₂ phase diagram in the main pipeline. After the valve opened, Tf2, Tf7, Tf9, Tf18 delivered the saturation curve successively. The phase of CO₂ transformed from gas-liquid to gaseous. In the test2 the time of maintenance in the gas-liquid saturation phase was longer than that of test1. Furthermore the characteristics of Tf3 and Tf4 evolution shows that the CO₂ entering the liquid phase in test2 was significantly more than test1. In general, an increase in the length of the vent pipe will cause the CO₂ front the valve to be in superheated phase and there were more liquid CO₂ generated behind valve.

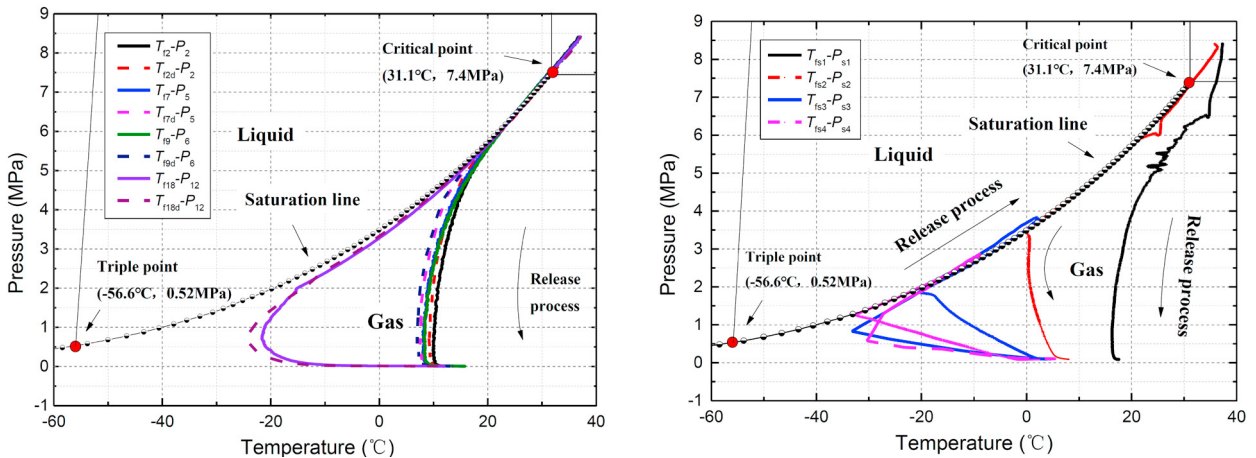


Fig. 4. Pressure-temperature developments in the main pipe and the vent pipe for test 2

3.1. Visible cloud of CO₂ dispersion

Fig. 5 shows the variations in the shape of CO₂ plume during the venting process. Observed the venting process, the variations in the shape of CO₂ plume can be divided into three stages: The first stage was rapid development of jet to complete expansion; the second stage was that the jet shape maintains a quasi-steady state; the third stage was the slow decay process of the jet. The duration of three stages was 5s, 15s and 392s respectively. After pneumatic valve opened, the supercritical CO₂ was venting into the air through the vent pipe during the first stage. In the second the scale of the visible cloud remains unchanged. The maximum width and height was 24m and 3m respectively. In the third stage the magnitude of CO₂ visible cloud continued to decay.

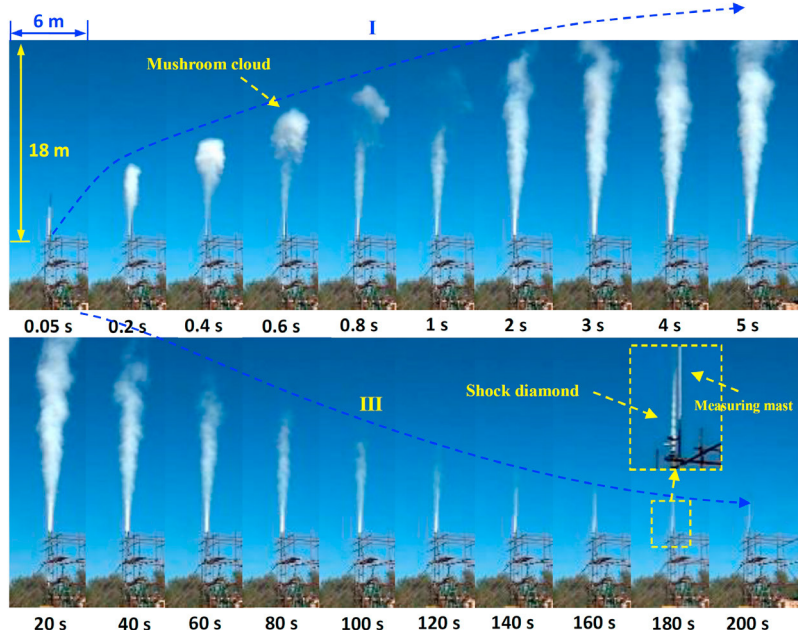


Fig. 5. Visible cloud development for test 1

4. Conclusions

According to the experimental study, some conclusions are demonstrated as follows:

(1) When a small diameter rupture occurred, a decompression wave propagated back and forth long the pipeline due to the rapid expansion of the high pressure CO₂ at the orifice. Passage of the decompression wave through the inventory caused pressure undershoot and rebound to a quasi-static level, this was accompanied by a sharp temperature drop and boiling nucleation.

(2) For the supercritical CO₂ test, the inventory transformed into a gas-liquid and then gas phase as the inventory pressure fell below P_e. A “two cold, intermediate hot” phenomenon was observed during the vertical leakage in the dense and supercritical release due to the dry ice particle accumulation near the orifice.

(3) For three phase CO₂ leakage, the gas-solid two-phase jet entrained a mass of dry ice particle, gaseous CO₂, air and condensed water in the near-field, this mixture continued to spread in the far-field. The intersection of the jet flow and settling CO₂ mixture resulted in complex visible cloud forms in dense CO₂ release.

Acknowledgement

The authors would like to acknowledge the funding received from the European Union Seventh Framework Programmes FP7-ENERGY-2009-1 under grant agreement number 241346 and FP7-ENERGY-2012-1STAGE under Grant agreement 309102.

References

- [1] Duan HB, Fan Y, Zhu L. What's the most cost-effective policy of CO₂ targeted reduction: an application of aggregated economic technological model with CCS [J]. *Appl Energ*, 2013, 112:866-75.
- [2] Chen ZA, Li Q, Liu LC, et al. A large national survey of public perceptions of CCS technology in China. *Appl Energy* 2015; 158:366–377.
- [3] Chong FK, Lawrence KK, Lim PP, et al. Planning of carbon capture storage deployment using process graph approach [J]. *Energy*, 2014, 76:641-651.
- [4] Knoope MMJ, Ramírez A, Faaij APC. Investing in CO₂ transport infrastructure under uncertainty: A comparison between ships and pipelines [J]. *Int J Greenh Gas Con*, 2015, 41:174-193.
- [5] ISO 13623. Petroleum and natural gas industries – pipeline transportation systems, 2nd Ed. 2009.
- [6] DNV-RP-J202. Design and operation of CO₂ pipelines. 2010.
- [7] CSA Z662. Oil and gas pipeline system. 2007.
- [8] Martynov S, Brown S, Mahgerefteh H, et al. Modelling three-phase releases of carbon dioxide from high-pressure pipelines [J]. *Int J Greenh Gas Con*, 2014, 92:36-46.
- [9] Aursand E, Dumoulin S, Hammer M, et al. Fracture propagation control in CO₂ pipelines: Validation of a coupled fluid–structure model [J]. *Engineering Structures*, 2016, 123:192-212.
- [10] Harper P, Wilday J, Bilio M. Assessment of the major hazard potential of carbon dioxide (CO₂) [J]. *Health and Safety Executive*, 2011, 1-28.
- [11] Koornneef J, Ramírez A, Turkenburg W, et al. The environmental impact and risk assessment of CO₂ capture, transport and storage - An evaluation of the knowledge base [J]. *Prog Energy Combust Sci*, 2012, 38: 62-86.
- [12] Mohitpour M, Jenkins A, Nahas G. A generalized overview of requirements for the design, construction, and operation of new pipelines for CO sequestration [J]. *Journal of Pipeline Engineering* 2008; 237-251. 2
- [13] Wareing CJ, Fairweather M, Falle SAEG, et al. Validation of a model of gas and dense phase CO₂ jet releases for carbon capture and storage application. *Int J Greenh Gas Con* 2014; 20:254-271.
- [14] Wen J, Heidari A, Xu BP et al. Dispersion of carbon dioxide from vertical vent and horizontal releases - A numerical study. *J Process Mechanical Engineering* 2013; 227:125-139.
- [15] Wareing CJ, Woolley RM, Fairweather M, et al. Large-scale validation of a numerical model of accidental releases from buried CO₂ pipelines. *Computer Aided Chemical Engineering* 2013, 32:229-234.
- [16] Han SH, Kim J, Chang D. An experimental investigation of liquid CO₂ release through a capillary tube [J]. *Energy Procedia*, 2013, 37:4724-4730.
- [17] Han SH, Chang D, Kim J, et al. Experimental investigation of the flow characteristics of jettisoning in a CO₂ carrier [J]. *Process Saf Environ*, 2014, 92:60-69.
- [18] Xie QY, Tu R, Jiang X, et al. The leakage behavior of supercritical CO₂ flow in an experimental pipeline system. *Appl Energy* 2014; 130:574-580.
- [19] Li K, Zhou XJ, Tu R, et al. The flow and heat transfer characteristics of supercritical CO₂ leakage from a pipeline. *Energy* 2014; 71:665-672.
- [20] Guo XL, Yan XQ, Yu JL, et al. Pressure response and phase transition in supercritical CO₂ releases from a large-scale pipeline. *Appl Energy* 2016; 178:189-197.
- [21] Guo XL, Yan XQ, Yu JL, et al. Pressure responses and phase transitions during the release of high pressure CO₂ from a large-scale pipeline. *Energy* 2016; 1-13.
- [22] Guo XL, Yan XQ, Yu JL, et al. Under-expanded jets and dispersion in supercritical CO₂ releases from a large-scale pipeline. *Appl Energy* 2016; 183:1279-1291.
- [23] Guo XL, Yan XQ, Yu JL, et al. Under-expanded jets and dispersions during the release of high pressure CO₂ from a large-scale pipeline [J]. *Energy*. 2016;119:53-66.